Joint Multitarget Detection and Tracking in Multipath Environment Using Expectation Maximization Algorithm

Zhihua Li, *Student Member, IEEE*, Hongtao Su, Xiao-Yang Liu, *Graduate Student Member, IEEE*, Guoqing Wang, and Mengdao Xing, *Fellow, IEEE*

***Abstract*—Joint detection and tracking is fundamentally important in signal processing, navigation, and radar applications. Especially, multitarget detection and tracking in multipath environments is a promising issue and broadening range for joint detection and tracking. However, its wide adoption in real-world systems is challenged by the unknown data association, complex and changeable motion environment, and data mutual coupling. To address those problems, we propose a joint detection and tracking scheme based on expectation maximization (EM) algorithm. By alternately computing the complete likelihood function and optimizing it with respect to target existence state (detection) and target kinematic state (tracking), the proposed scheme iteratively optimizes estimation and data association. Furthermore, we provide a hybrid forward and backward algorithm during the M-step to deal with the coupling of the target existence state and target kinematic state. We also provide a convergence speed-up algorithm based on K-means method and stochastic initialization method to accelerate convergence speed. Finally, we verify the effectiveness of the proposed joint detection and tracking scheme by conducting extensive simulations with different tracking scenarios. The simulation results show that the proposed algorithm not only improves the detection and tracking performance, but also stays stable performance in complex and changeable motion environment and high noise background.**

***Index Terms*—Expectation-maximization (EM), joint detection and estimation, multipath, terms-multitarget.**

I. Introduction

MULTITARGET detection and tracking, which includes estimation of targets existence states and estimation of target kinematic states, is a basic problem in the area of maritime reconnaissance, drug enforcement, and traffic control [1]–[3]. Most multitarget detection and tracking algorithms are assumed that one target generates only one measurement in a single scan with detection probability less than unity [4]–[6]. However, the situation that multiple measurements generated by one target in one scan often occur due to, such as multipath propagation phenomenon in underwater sound transmission or sky-wave over-the-horizon radar (OTHR), multipath effects in millimeter-wave wireless communication or extended nature of targets with a high resolution radar [7]–[9]. This kind of sensing problem is called joint detection and tracking of multitarget and multipath (MTMP-JDT) problem in this article.

There are two potential advantages for the MTMP system compared with single-target and single-path pattern. The first one can be regarded as sensitivity, which refers to the ability to detect or track targets with high noise background. MTMP-JDT system can extract more targets information from multipath returns, which increases the total energy received from the targets. Combining these multiple pieces of information can enhance the signal-to-noise ratio (SNR), which further improved the system's sensitivity. The second advantage can be referred to as continuity, which is the ability to obtain a continuous maneuvering state of the targets. Poor continuity refers to that the tracks drop out in the complex motion environment, such as loss of maneuver handling, emergency braking, or target cluster with various maneuvering parts. The MTMP-JDT can provide robustness against signal fluctuation. In this situation, tracks or detection on different paths or different parts of a target cluster would not drop out simultaneously, and a set of tracks can maintain continuity. In general, trackers will be more successful in associating a cluster of returns in a predictable pattern.

Three challenges are needed to face for the MTMP-JDT issue: 1) Unknown data association: The measurement needs to be associated with the target; Apart from that, the measurement scattered from target needs to be associated with the propagation path. We call it the triple target-to-path-measurement association event in this article. 2) Complex and changeable motion environment: The number of targets varies over time and is unknown. In addition, targets may appear and disappear anytime and anywhere without prior information. 3) Coupling of detection, estimation, and identification: Target existence state, the target-to-path-measurement association, and target kinematic state are tightly coupled.

Manuscript received May 31, 2021; revised August 7, 2021; accepted September 20, 2021. Date of publication September 30, 2021; date of current version October 21, 2021. This work was supported in part by the National Natural Science Foundation of China under Grants 61372134 and 62003348 and in part by the Natural Science Foundation of Jiangsu Province under Grant BK20200633. *(Corresponding author: Hongtao Su.)*

Zhihua Li and Hongtao Su are with the National Laboratory of Radar Signal Processing, Xidian University, Xi'an 710071, China (e-mail: lzhxdstu@126.com; suht@xidian.edu.cn).

Xiao-Yang Liu is with the Department of Electrical Engineering, Columbia University, New York, NY 10027 USA (e-mail: xl2427@columbia.edu).

Guoqing Wang is with the School of Information and Control Engineering, China University of Mining and Technology, Xuzhou 221116, China (e-mail: guoqingwang@cumt.edu.cn).

Mengdao Xing is with the Academy of Advanced Interdisciplinary Research, Xidian University, Xi'an 710071, China (e-mail: xmd@xidian.edu.cn).

Digital Object Identifier 10.1109/JSTARS.2021.3116798

Plenty works have been done aiming to solve the MTMP-JDT problem. Based on measurement level fusion, Davey *et al.* gave a joint detection and tracking method in [10]. One step further, Davey *et al.* also proposed a mode-ware detection tracking algorithm by approximate the detection results based on the probabilistic multihypothesis tracker (PMHT) [11]–[13]. However, detection and tracking performance under those techniques are poor and specially in high noise background. Based on the joint probabilistic data association (JPDA) method [15], [16], Habtemariam *et al.* proposed the multiple-detection JPDA Filter (MD-JPDAF) [14]. Using the multiple hypothesis tracker (MHT) framework [17], the multiple detection MHT (MD-MHT) [18] is presented. Fusing all the available measurement information as much as possible, the above methods gain an effective multitarget tracking performance. Tang *et al.* proposed a multiple-detection PHD (MD-PHD) in [19] by extending standard PHD filter to multidetection situation. These measurement-level fusion algorithms can achieve remarkable tracking performance over the first category tracking algorithms. Another category is based on closed-loop iterative processing. Laet *et al.* gave the solution to the tracking without known association by using the variational Bayesian approach [20]. Furthermore, Lan *et al.* extended the variational bayesian approach to the MTMP case and proposed the JDT-VB algorithm [21]. One drawback of the variational Bayesian based algorithms is that they suffer from computational complexity when there is not proper initialization, such as single element subsets initialization, which may cause performance degradation. These iterative methods are attractive and effective for decoupling of association and estimation. Some advanced deep learning methods [22], [23] are devoted to solving the multitarget tracking and incomplete data problem, which is novelty, attractable and can be used in future work.

The expectation maximization (EM) algorithm is an effectively iterative optimization approach to compute maximum likelihood estimates, useful in the presence of incomplete data [24]. Akinin *et al.* aimed to tackle pattern recognition on satellite images by presenting a new EM image segmentation method [25]. Einicke *et al.* adopted K-means algorithm as the initial setting for clustering results to speed up the convergence of EM algorithm [26]. Lan *et al.* [27] based on sliding window and structure of parallel proposed a computation efficient scheme to address the OTHR target tracking problem. To the best of our knowledge, no one has dealt with the joint detection and tracking of multitarget multipath problem by utilizing EM framework, which is attractive to cope with the three challenges mentioned above.

In this article, an efficient joint multitarget detection and tracking algorithm (JMDT-EM) is proposed in multipath environment. Our investigation is capable of solving detection, tracking, and data association at the same time and is durable under complex and changeable motion environment and low SNR circumstance. First, the proposed JMDT-EM algorithm is investigated alternating calculating the log-likelihood function based on the probability density function (PDF) of missing data (target-to-path-to-measurement association) in E-Step and optimizing the log-likelihood function on the system parameters (desired target existence state and kinematic state) in M-Step. More importantly, utilizing the iterative mechanism, the closed loop between data association and state estimation is established, which is effective to solve the coupling problem between data association and target state estimation. Second, a hybrid forward and backward algorithm is provided during target existence estimation and target state estimation to solve the coupling of target existence state and target estimation state. Third, a convergence speed up algorithm based on K-means strategy and stochastic initialization strategy is also provided to accelerate convergence speed. Simulation results demonstrate that the JMDT-EM algorithm not only obtains a good detection and tracking performance, but also stays stable performance in complex and changeable motion environment and low SNR circumstance.

The rest of this article is organized as follows. Section II gives the problem formulation of joint multitarget multipath detection and tracking system. Section III discusses and develops the JMDT-EM algorithm for target state estimation and data association. Section IV presents the simulation results. Finally, Section V concludes this article.

II. Problem Formulation

System model used for problem formulation and algorithm design are described in this section. Section II-A gives target kinematic state model and target existence state model. Section II-B presents the measurement model. Specially, the definition of data association event between target state, measurement, and propagation mode is given in Definition 2.1. Finally, Section II-C gives the problem formulation.

A. Target Kinematic State Model and Target Existence State Model

Let T_k be the known number of possible targets that appear in the surveillance region at time instant k. Denote $\boldsymbol{X}_k = \{\boldsymbol{x}_{t,k}\}_{t=1}^{T_k}$ as the set of targets kinematic states. The target dynamical equation is given

$$\boldsymbol{x}_{t,k} = \boldsymbol{f}_t\left(\boldsymbol{x}_{t,k-1}\right) + \boldsymbol{v}_{t,k-1}, t = 1, \ldots, T_k \tag{1}$$

where $\boldsymbol{f}_t(\cdot)$ is the state transition function, $\boldsymbol{v}_{t,k-1}$ is a white Gaussian noise with zero mean and covariance $\boldsymbol{Q}_{t,k-1}$.

Define $\boldsymbol{S}_k = \{s_{t,k}\}_{t=1}^{T_k}$ as the set of target existence state with $s_{t,k} \in \{0, 1\}$ denoting the detectable state of target t at time instant k. Target t is detectable at time k if $s_{t,k} = 1$, and is alternatively undetectable if $s_{t,k} = 0$. Target existence state $s_{t,k}$ evolves following a two-state Markov process with $p(s_{t,k} = a | s_{t,k-1} = b)$, $\forall a, b \in \{0, 1\}$ being the known transition probability.

B. Measurement Model

Assume that I is the number of valid propagation modes. p_d^i is the detection probability of a target through the ith $(i = 1, \ldots, I)$ propagation mode. Let N_k be the known number of measurements at time instant k. $\boldsymbol{Z}_k = \{\boldsymbol{z}_{n,k}\}_{n=1}^{N_k}$ is denoted as the measurement set. For the nth measurement $\boldsymbol{z}_{n,k}$ is either originated from target or from clutter. The target-originated

measurement $\boldsymbol{z}_k$ is described as

$$\boldsymbol{z}_k = \boldsymbol{h}_i(\boldsymbol{x}_k) + \boldsymbol{w}_{i,k}, \quad i = 1, 2, \ldots, I \tag{2}$$

where $\boldsymbol{h}_i(\cdot)$ is the measurement function of the ith propagation mode, $\boldsymbol{w}_{i,k}$ is the measurement noise, following Gaussian distribution with zero-mean and covariances $\boldsymbol{R}_{i,k}$.

The clutter-originated measurement (false measurement) is modeled as a uniform clutter PDF $p_c(\boldsymbol{z})$ with a Poisson probability mass function $\mu_c(n)$ in the corresponding region G_k with the corresponding volume V_{G_k}

$$p_c(\boldsymbol{z}_k) = \begin{cases} V_{G_k}^{-1} \text{if} & \boldsymbol{z}_k \in G_k, \\ 0 & \text{otherwise}, \end{cases} \tag{3}$$

$$\mu_c(n) = \frac{(\lambda V_{G_k})^n e^{-\lambda V_{G_k}}}{n!}, n = 0, 1, 2, \ldots \tag{4}$$

with λ being the spatial density of the clutter, taken as N_k/V_{G_k}.

C. Problem Formulation

Definition 2.1: Define the multitarget multipath data association event among targets, multipath propagation modes and measurements at time instant k as $\boldsymbol{\Theta}_k = \boldsymbol{\theta}'_k \cup \boldsymbol{\theta}''_k \cup \boldsymbol{\theta}'''_k$.

- $\boldsymbol{\theta}'_k = \{\theta_k^{t,i,n}\}_{t=1,i=1,n=1}^{T_k,I,N_k}$ represent the targets exist, and the nth measurement is originated from the tth target via the ith propagation mode;
- $\boldsymbol{\theta}''_k = \{\theta_k^{t,i,0}\}_{t=1,i=1}^{T_k,I}$ represent the tth target is not detectable by the ith propagation mode;
- $\boldsymbol{\theta}'''_k = \{\theta_k^{0,0,n}\}_{n=1}^{N_k}$ represent the nth measurement is scattered from clutter and irrelevant to any propagation modes or targets.

A joint event $\boldsymbol{\Theta}_k$ is feasible only if it satisfies the following assumptions: 1) A measurement either scattered from one underlying target or from false clutter at one time instant. 2) A target via a specific propagation mode is either not detectable or generates only one measurement at one time instant.

Denote $[k-l, k] = \{k-l, k-l+1, \ldots, k\}$ as the time interval, where l denotes the window length. Denote the sequences of sets $\boldsymbol{S}_{k-l}^k = \{\boldsymbol{S}_j\}_{j=k-l}^k$, $\boldsymbol{X}_{k-l}^k = \{\boldsymbol{X}_j\}_{k=j-l}^K$, $\boldsymbol{Z}_{k-l}^k = \{\boldsymbol{Z}_j\}_{j=k-l}^k$ and $\boldsymbol{\Theta}_{k-l}^k = \{\boldsymbol{\Theta}_j\}_{j=k-l}^k$ as the collections of target existence state, targets kinematic state, measurements, and data association events, respectively.

Based on the models of target existence state, target kinematic state, and multipath measurements, the problem of multitarget detection and tracking in multipath environment is aimed to obtain target existence state $\boldsymbol{S}_{k-l}^k$ (detection) and target kinematic state $\boldsymbol{X}_{k-l}^k$ (tracking), using measurements $\boldsymbol{Z}_{k-l}^k$ with unknown data association event $\boldsymbol{\Theta}_{k-l}^k$ among targets, propagation modes, and measurements, i.e.,

$$\mathbf{P1}: p(\boldsymbol{X}_{k-l}^k | \boldsymbol{Z}_{k-l}^k) = \sum_{\boldsymbol{\Theta}_{k-l}^k} p\left(\boldsymbol{X}_{k-l}^k | \boldsymbol{Z}_{k-l}^k, \boldsymbol{\Theta}_{k-l}^k\right) \tag{5}$$

$$p(\boldsymbol{S}_{k-l}^k | \boldsymbol{Z}_{k-l}^k) = \sum_{\boldsymbol{\Theta}_{k-l}^k} p\left(\boldsymbol{S}_{k-l}^k | \boldsymbol{Z}_{k-l}^k, \boldsymbol{\Theta}_{k-l}^k\right). \tag{6}$$

To solve problem **P1**, there are some difficulties that should be considered:

1) An efficient method for solving incomplete data is needed. To estimate the target existence state $\boldsymbol{S}_{k-l}^k$ and the target kinematic state $\boldsymbol{X}_{k-l}^k$, the multipath data association $\boldsymbol{\Theta}_{k-l}^k$ among targets, propagation modes and the measurements $\boldsymbol{Z}_{k-l}^k$ should be known as a priori. However, the missing of the data association event $\boldsymbol{\Theta}_{k-l}^k$ lead to the multipath multitarget detection and tracking as an *incomplete data* estimation problem.
2) An iterative optimization is needed. The coupling of target existence state estimation $\boldsymbol{S}_{k-l}^k$ and target kinematic state estimation $\boldsymbol{X}_{k-l}^k$ leads to the necessary of an effective method for identification and estimation.

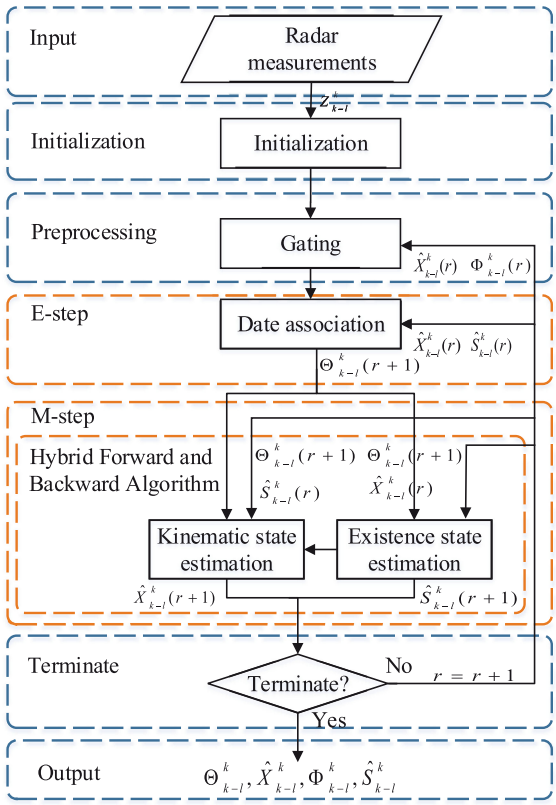

Fig. 1. Information flow of the proposed JMDT-EM algorithm.

The EM algorithm is an iterative optimization procedure to tackle with maximum likelihood parameter estimation problem with incomplete data. The well-known probabilistic data association tracker and the PMHT are widely used to solve the joint target detection and tracking problem. While, in this article, we propose the JMDT-EM algorithm, based on the EM framework, to solve the problem of joint target detection and tracking in a MTMP propagation environment.

III. Joint Multitarget Detection and Tracking

We first outline some notations for computational and sampling complexity. Then, the information flow of the proposed JMDT-EM algorithm is given in Fig. 1. The framework of the JMDT-EM algorithm is presented in Section III-A. The main components of the JMDT-EM algorithm are described in detail in Sections III-B and III-C. Finally, the initialization and termination are discussed in Section III-D.

Definition 3.1: Define the log-likelihood function $\mathcal{L}_{k-l}^{k}$ and the $\mathcal{Q}$-function as

$$\mathcal{L}_{k-l}^{k} = \log p\left(\boldsymbol{X}_{k-l}^{k}, \boldsymbol{S}_{k-1}^{k}, \boldsymbol{\Theta}_{k-l}^{k}, \boldsymbol{Z}_{k-l}^{k} | \boldsymbol{Z}_{1}^{k-l-1}\right) \quad (7)$$

$$\mathcal{Q}_{k-l}^{k}(r) = \mathbb{E}\left(\mathcal{L}_{k-l}^{k} | \boldsymbol{Z}_{k-l}^{k}, \widehat{\boldsymbol{X}}_{k-l}^{k}(r), \widehat{\boldsymbol{S}}_{k-l}^{k}(r)\right) \quad (8)$$

where $\widehat{\boldsymbol{X}}_{k-l}^{k}(r)$ and $\widehat{\boldsymbol{S}}_{k-l}^{k}(r)$ are the rth iteration cycle estimation of target existence state $\boldsymbol{S}_{k-l}^{k}$ and target kinematic state $\boldsymbol{X}_{k-l}^{k}$, respectively.

Definition 3.2: Define the posterior probability $\varpi_{j}^{(r)}(t,i,n)$ of the association event, the prior probability $\lambda_{j}^{(r)}(t,i,n)$ of the association event and the observation merit function $\xi_{j}^{(r)}(t,i,n)$ at jth time instant and rth iteration cycle as

$$\varpi_{j}^{(r)}(t,i,n) \triangleq p\left(\theta_{j}^{t,i,n} \left| \boldsymbol{Z}_{k-l}^{k}, \widehat{\boldsymbol{X}}_{k-l}^{k}(r), \widehat{\boldsymbol{S}}_{k-l}^{k}(r)\right.\right) \quad (9)$$

$$\lambda_{j}^{(r)}(t,i,n) \triangleq p\left(\theta_{j}^{t,i,n} | s_{t,j}, \boldsymbol{x}_{t,j}, \boldsymbol{z}_{t,j}\right) \quad (10)$$

$$\xi_{j}^{(r)}(t,i,n) \triangleq p\left(\boldsymbol{z}_{n,j} \left| \theta_{j}^{t,i,n}, s_{t,j}, \boldsymbol{x}_{t,j}\right.\right). \quad (11)$$

A. Framework of the Proposed JMDT-EM Algorithm

The proposed JMDT-EM algorithm mainly contains two iterative steps [26], [27].

E-step

$$\mathcal{Q}_{k-l}^{k}(r) = \mathbb{E}\left(\mathcal{L}_{k-l}^{k} | \boldsymbol{Z}_{k-l}^{k}, \widehat{\boldsymbol{X}}_{k-l}^{k}(r), \widehat{\boldsymbol{S}}_{k-l}^{k}(r)\right). \quad (12)$$

M-step

$$\left\{\widehat{\boldsymbol{X}}_{k-l}^{k}(r+1), \widehat{\boldsymbol{S}}_{k-l}^{k}(r+1)\right\} = \underset{\boldsymbol{X}_{k-l}^{k}, \boldsymbol{S}_{k-1}^{k}}{\arg\max}\ \mathcal{Q}_{k-l}^{k}(r) \quad (13)$$

where r denotes the rth iteration cycle. The E-step is engaged to calculate the conditional expectation for the data association $\boldsymbol{\Theta}_{k-l}^{k}$ using the current estimation of target existence state $\widehat{\boldsymbol{S}}_{k-l}^{k}(r)$ and kinematic state $\widehat{\boldsymbol{X}}_{k-l}^{k}(r)$ and measurements $\boldsymbol{Z}_{k-l}^{k}$. The M-step provides an updated estimations of target existence state $\widehat{\boldsymbol{S}}_{k-l}^{k}(r+1)$ and target kinematic state $\widehat{\boldsymbol{X}}_{k-l}^{k}(r+1)$ through maximizing $\mathcal{Q}$-function $\mathcal{Q}_{k-l}^{k}(r)$. Furthermore, a hybrid forward and backward algorithm for tackle the coupling of target existence state and target kinematic state is provided during M-step.

B. Preprocessing

In order to eliminate highly infeasible association hypothesis events among targets, propagation modes, and measurements, gating technique is often used, which can further reduce the computational cost. The validation region is an $n_{\boldsymbol{z}}$-dimensional ellipse, which is defined as follows:

$$V_{t,i,k}(\eta) := \{\boldsymbol{z}_{n,k} \in \boldsymbol{Z}_{k} : \mathbf{D}(\boldsymbol{z}_{n,k} - \widehat{\boldsymbol{z}}_{t,i,k}, \boldsymbol{P}_{t,i,k}) \leq \eta\} \quad (14)$$

where $n_{\boldsymbol{z}}$ is the dimension of the candidate measurement, $\widehat{\boldsymbol{z}}_{t,i,k} = \boldsymbol{h}_{i}(\widehat{\boldsymbol{x}}_{t,k})$ is the predicted measurement, $\boldsymbol{P}_{t,i,k} = \boldsymbol{R}_{i,k} + \boldsymbol{H}_{i}\widehat{\boldsymbol{\Phi}}_{t,k}(\boldsymbol{H}_{i})^{T}$ is the associated innovation covariance and $[\cdot]^{T}$ denotes transpose operations of a matrix. $\widehat{\boldsymbol{x}}_{t,k}$, $\widehat{\boldsymbol{\Phi}}_{t,k}$ denote the target kinematic state estimation and the corresponding covariance, respectively. $\boldsymbol{H}_{i}$ denotes the Jacobian matrix of $\boldsymbol{h}_{i}$. $\mathbf{D}(\cdot)$ represents Mahalanobis distance defined by $\mathbf{D}(\boldsymbol{x}, \boldsymbol{\Sigma}) = \boldsymbol{x}^{T}\boldsymbol{\Sigma}^{-1}\boldsymbol{x}$. $\boldsymbol{\Sigma}^{-1}$ denotes a positive-definite matrix. $[\cdot]^{-1}$ denotes the inverse operations of a matrix. The constant η is predetermined to guarantee gate probability equal to p_{g}. Define the union of valid region for all targets as the valid region for measurements and the valid volume V_{k} can be approximated by

$$V_{k} \approx \bigcup_{t=1}^{N_{k}} \max\{V_{t,1,k}, \ldots, V_{t,I,k}\}. \quad (15)$$

C. Key Routines

1) E-Step: The log-likelihood function $\mathcal{L}_{k-l}^{k}$ defined in (7) has the following calculation expression:

$$\mathcal{L}_{k-l}^{k} = \mathcal{L}_{1,k-l}^{k} + \mathcal{L}_{2,k-l}^{k} + \mathcal{L}_{3,k-l}^{k} + \mathcal{L}_{4,k-l}^{k} \quad (16)$$

with

$$\mathcal{L}_{1,k-l}^{k} = -\frac{1}{2}\sum_{j=k-l}^{k}\sum_{t=1}^{T_{j}} \log\left(\left|2\pi\boldsymbol{Q}_{t,j}\right|\right) - \frac{1}{2}\sum_{j=k-l}^{k}\sum_{t=1}^{T_{j}} \mathbf{D}\left(\boldsymbol{x}_{t,j} - \boldsymbol{f}\left(\boldsymbol{x}_{t,j-1}\right), \boldsymbol{Q}_{t,j}\right) \quad (17)$$

$$\mathcal{L}_{2,k-l}^{k} = -\frac{1}{2}\sum_{t=1}^{T_{\varsigma}} \log\left(\left|2\pi\boldsymbol{\Sigma}_{t,\varsigma,\varsigma|1:\varsigma}\right|\right) - \frac{1}{2}\sum_{t=1}^{T_{\varsigma}} \mathbf{D}\left(\boldsymbol{x}_{t,\varsigma} - \widehat{\boldsymbol{x}}_{t,\varsigma|1:\varsigma}, \boldsymbol{\Sigma}_{t,\varsigma,\varsigma|1:\varsigma}\right) \quad (18)$$

$$\mathcal{L}_{3,k-l}^{k} = -\frac{1}{2}\sum_{j=k-l}^{k}\sum_{t=1}^{T_{j}} \left(\log\left(\left|2\pi\boldsymbol{R}_{i,j}\right|\right) + \mathbf{D}\left(\boldsymbol{z}_{j} - \boldsymbol{h}_{i}\left(\boldsymbol{x}_{t,j}\right), \boldsymbol{R}_{i,j}\right)\right) + \sum_{j=k-l}^{k}\left(N_{j} - \sum_{t=1}^{T_{j}}\sum_{i=1}^{I} d^{t,i}\left(\boldsymbol{\Theta}_{j}\right)\right)\log\left(V_{j}\right), \theta_{j}^{t,i,n} \in \boldsymbol{\theta}'_{j} \quad (19)$$

$$\mathcal{L}_{4,k-l}^{k} = \sum_{j=k-l}^{k} \log p(\boldsymbol{\Theta}_{j}|\boldsymbol{s}_{j}) + \sum_{j=k-l}^{k} \log p\left(\boldsymbol{s}_{j}|\boldsymbol{s}_{j-1}\right) + \log p(\boldsymbol{s}_{\varsigma}) \quad (20)$$

where $\varsigma = k - l - 1$, and

$$p(\boldsymbol{\Theta}_{j}|\boldsymbol{s}_{j}) = \frac{(\lambda V_{j})^{\left(N_{j} - \sum_{t=1}^{T_{j}}\sum_{i=1}^{I} d^{t,i}(\boldsymbol{\Theta}_{j})\right)}}{N_{j}!}\exp(-\lambda V_{j}) \times \prod_{t=1}^{T_{j}}\prod_{i=1}^{I}\left(p_{d}^{i}(s_{t,j})\right)^{d_{j}^{t,i}(\boldsymbol{\Theta}_{j})}\left(1 - p_{d}^{i}(s_{t,j})\right)^{1 - d_{j}^{t,i}(\boldsymbol{\Theta}_{j})} \quad (21)$$

$d^{t,i}(\boldsymbol{\Theta}_{j})$ is the detection indicator that refers to whether a measurement is scattered from target t via path i in $\boldsymbol{\Theta}_{j}$. $p_{d}^{i}(s_{t,k})$ denotes the target detection probability for each target t via each propagation path i.

Proof: See Appendix A.

The $\mathcal{Q}$-function $\mathcal{Q}_{k-l}^{k}(r)$ defined in (8) is given as follows:

$$\mathcal{Q}_{k-l}^{k}(r) = \mathcal{Q}_{1,k-l}^{k} + \mathcal{Q}_{2,k-l}^{k} + \mathcal{Q}_{3,k-l}^{k} + \mathcal{Q}_{4,k-l}^{k} \tag{22}$$

with

$$\begin{aligned}\mathcal{Q}_{1,k-l}^{k} &= \mathbb{E}\left(\mathcal{L}_{1,k-l}^{k}|\boldsymbol{Z}_{k-l}^{k}, \widehat{\boldsymbol{X}}_{k-l}^{k}(r), \widehat{\boldsymbol{S}}_{k-l}^{k}(r)\right) \\ &= -\frac{1}{2}\sum_{j=k-l}^{k}\sum_{t=1}^{T_j}\log\left(\left|2\pi\boldsymbol{Q}_{t,j}\right|\right) \\ &\quad -\frac{1}{2}\sum_{j=k-l}^{k}\sum_{t=1}^{T_j}\mathbf{D}\left(\boldsymbol{x}_{t,j} - \boldsymbol{f}_t\left(\boldsymbol{x}_{t,j-1}\right), \boldsymbol{Q}_{t,j}\right)\end{aligned} \tag{23}$$

$$\begin{aligned}\mathcal{Q}_{2,k-l}^{k} &= \mathbb{E}\left(\mathcal{L}_{2,k-l}^{k}|\boldsymbol{Z}_{k-l}^{k}, \widehat{\boldsymbol{X}}_{k-l}^{k}(r), \widehat{\boldsymbol{S}}_{k-l}^{k}(r)\right) \\ &= -\frac{1}{2}\sum_{t=1}^{T_\varsigma}\log\left(\left|2\pi\boldsymbol{\Sigma}_{t,\varsigma,\varsigma|1:\varsigma}\right|\right) \\ &\quad -\frac{1}{2}\sum_{t=1}^{T_\varsigma}\mathbf{D}\left(\boldsymbol{x}_{t,\varsigma} - \widehat{\boldsymbol{x}}_{t,\varsigma|1:\varsigma}, \boldsymbol{\Sigma}_{t,\varsigma,\varsigma|1:\varsigma}\right)\end{aligned} \tag{24}$$

$$\begin{aligned}\mathcal{Q}_{3,k-l}^{k} &= \mathbb{E}\left(\mathcal{L}_{3,k-l}^{k}|\boldsymbol{Z}_{k-l}^{k}, \widehat{\boldsymbol{X}}_{k-l}^{k}(r), \widehat{\boldsymbol{S}}_{k-l}^{k}(r)\right) \\ &= \Bigg(-\frac{1}{2}\sum_{j=k-l}^{k}\sum_{t=1}^{T_j}\sum_{i=1}^{I}\sum_{n:\boldsymbol{z}_{n,j}\in V_j(\eta)} \\ &\quad \left(\log\left(|2\pi\boldsymbol{R}_{i,j}|\right) + \mathbf{D}\left(\boldsymbol{z}_j - \boldsymbol{h}_i\left(\boldsymbol{x}_{t,j}\right), \boldsymbol{R}_{i,j}\right)\right) \\ &\quad + \sum_{j=k-l}^{k}\left(1-\delta(\boldsymbol{\Theta}_j)\right)\log\left(V_j\right)\Bigg) \\ &\quad \times p\left(\theta_j^{t,i,n} \in \boldsymbol{\theta}_j'|\boldsymbol{Z}_{k-l}^{k}, \widehat{\boldsymbol{X}}_{k-l}^{k}(r), \widehat{\boldsymbol{S}}_{k-l}^{k}(r)\right)\end{aligned} \tag{25}$$

$$\begin{aligned}\mathcal{Q}_{4,k-l}^{k} = &\sum_{j=k-l}^{k}\log p(\boldsymbol{\Theta}_j|\boldsymbol{s}_j) + \sum_{j=k-l}^{k}\log p\left(\boldsymbol{s}_j|\boldsymbol{s}_{j-1}\right) \\ &+ \log p(\boldsymbol{s}_\varsigma).\end{aligned} \tag{26}$$

Proof: See Appendix B.

2) M-Step: To get the $\mathcal{Q}$-function $\mathcal{Q}_{k-l}^{k}(r)$, it is important to obtain the posterior probability $\varpi_j^{(r)}(t,i,n)$ defined in (9) which can be calculated by Bayes rule

$$\begin{aligned}\varpi_j^{(r)}(t,i,n) &= p\left(\theta_j^{t,i,n} \in \boldsymbol{\theta}_j'|\boldsymbol{Z}_{k-l}^{k}, \widehat{\boldsymbol{X}}_{k-l}^{k}(r), \widehat{\boldsymbol{S}}_{k-l}^{k}(r)\right) \\ &= \frac{\lambda\!\!\!^{-}_j^{(r)}(t,i,n)\xi_j^{(r)}(t,i,n)}{\sum_{t=1}^{T_j}\sum_{i=1}^{I}\sum_{n:\boldsymbol{z}_{n,j}\in V_j(\eta)}\lambda\!\!\!^{-}_j^{(r)}(t,i,n)\xi_j^{(r)}(t,i,n)}\end{aligned} \tag{27}$$

with

$$\begin{aligned}\lambda_j^{(r)}(t,i,n) &= p\left(\theta_j^{t,i,n}|s_{t,j}, \boldsymbol{x}_{t,j}, \boldsymbol{z}_{t,j}\right) \\ &= \frac{(\lambda V_j)^{N_C(\boldsymbol{\Theta}_j)}}{N_j!}\exp(-\lambda V_j) \\ &\quad \left(p_d^i(s_{t,j})\right)^{d_j^{t,i}(\boldsymbol{\Theta}_j)}\left(1-p_d^i(s_{t,j})\right)^{1-d_j^{t,i}(\boldsymbol{\Theta}_j)}\end{aligned} \tag{28}$$

$$\begin{aligned}\xi_j^{(r)}(t,i,n) &= p\left(\boldsymbol{z}_j\left|\theta_j^{t,i,n}, \boldsymbol{x}_{t,j}, s_{t,j}\right.\right) \\ &= \mathcal{N}\left(\boldsymbol{z}_{n,j}\left(d_j^{t,i}(\boldsymbol{\Theta}_j)\right); \boldsymbol{h}_i(\boldsymbol{x}_{t,j}), \boldsymbol{R}_{i,j}\right)\end{aligned} \tag{29}$$

where $\mathcal{N}(\boldsymbol{x};\mu,\boldsymbol{\delta})$ represents the Gaussian probability function of $\boldsymbol{x}$ with mean μ and covariance $\boldsymbol{\delta}$.

Then, a virtual measurement $\tilde{\boldsymbol{z}}_j^{t,i}(r)$ associated with the tth target and ith propagation mode and the corresponding synthetic-covariance $\tilde{\boldsymbol{R}}_j^{t,i}(r)$ are given by

$$\tilde{\boldsymbol{z}}_j^{t,i}(r) = \frac{\sum_{n:\boldsymbol{z}_{n,j}\in V_j(\eta)}\left(\varpi_j^{(r)}(t,i,n)\boldsymbol{z}_{n,j}\right)}{\sum_{n:\boldsymbol{z}_{n,j}\in V_j(\eta)}\varpi_j^{(r)}(t,i,n)} \tag{30}$$

$$\left(\tilde{\boldsymbol{R}}_j^{t,i}(r)\right)^{-1} = \left(\boldsymbol{R}_j^{t,i}\right)^{-1}\left(\sum_{n:\boldsymbol{z}_{n,j}\in V_j(\eta)}\varpi_j^{(r)}(t,i,n_j)\right). \tag{31}$$

Through putting (27), (30)–(31) into (22), followed by some simple algebraic manipulations, the $\mathcal{Q}$-function $\mathcal{Q}_{k-l}^{k}(r)$ is rewritten as

$$\begin{aligned}&\mathcal{Q}_{k-l}^{k}(r) = \\ &-\frac{1}{2}\sum_{j=k-l}^{k}\sum_{t=1}^{T_j}\sum_{i=1}^{I}\mathbf{D}\left(\tilde{\boldsymbol{z}}_j^{t,i}(r)\text{–}\boldsymbol{h}_i(\boldsymbol{x}_{t,j}), \tilde{\boldsymbol{R}}_j^{t,i}(r)\right)\varpi_j^{(r)}(t.i) \\ &-\frac{1}{2}\sum_{j=k-l}^{k}\sum_{t=1}^{T_j}\mathbf{D}\left(\boldsymbol{x}_{t,j} - \boldsymbol{f}_t\left(\boldsymbol{x}_{t,j-1}\right), \boldsymbol{Q}_{t,j}\right) \\ &-\frac{1}{2}\sum_{t=1}^{T_j}\mathbf{D}\left(\boldsymbol{x}_{t,\varsigma} - \widehat{\boldsymbol{x}}_{t,\varsigma|1:\varsigma}, \boldsymbol{\Sigma}_{t,\varsigma,\varsigma|1:\varsigma}\right) \\ &+\sum_{j=k-l}^{k}\sum_{t=1}^{T_j}\sum_{i=1}^{I}\log\Bigg(\frac{(\lambda V_j)^{N_C(\boldsymbol{\Theta}_j)}}{N_j!}\exp(-\lambda V_j) \\ &\quad \left(p_d^i(s_{t,j})\right)^{d_j^{t,i}(\boldsymbol{\Theta}_j)}\left(1-p_d^i(s_{t,j})\right)^{1-d_j^{t,i}(\boldsymbol{\Theta}_j)}\Bigg) \\ &+\sum_{j=k-l}^{k}\sum_{t=1}^{T_j}\log p\left(s_{t,j}|s_{t,j-1}\right) + \sum_{t=1}^{T_j}\log p(s_{t,\varsigma})\end{aligned} \tag{32}$$

with

$$\varpi_j^{(r)}(t,i) = \sum_{n:\boldsymbol{z}_{n,j}\in V_j(\eta)}\varpi_j^{(r)}(t,i,n) \tag{33}$$

representing the *posteriori* probability of the association event which involves the tth target and ith propagation mode corresponding to rth iteration cycle.

Furthermore, on equating the derivative of the right hand of (32) with respect to $\boldsymbol{X}_{k-l}^{k}$ and $\boldsymbol{S}_{k-l}^{k}$ to zero, the MAP state

estimate of $\widehat{\boldsymbol{X}}_{k-l}^{k}(r+1)$ and $\widehat{\boldsymbol{S}}_{k-l}^{k}(r+1)$ is used here

$$\begin{aligned}
&\sum_{t=1}^{T_j}\sum_{i=1}^{I}\log\left(\frac{(\lambda V_j)^{N_C(\boldsymbol{\Theta}_j)}}{N_j!}\exp(-\lambda V_j)\right.\\
&\left.\times\left(p_d^i(s_{t,i})\right)^{d_j^{t,i}(\boldsymbol{\Theta}_j)}\left(1-p_d^i(s_{t,i})\right)^{1-d_j^{t,i}(\boldsymbol{\Theta}_j)}\right)\\
&-\frac{1}{2}\sum_{t=1}^{T_j}\sum_{i=1}^{I}\left(\boldsymbol{H}_i(\boldsymbol{x}_{t,j})\right)^T\left(\tilde{\boldsymbol{R}}_j^{t,i}(r)\right)^{-1}\\
&\times\left(\tilde{\boldsymbol{z}}_j^{t,i}(r)-\boldsymbol{h}_i(\boldsymbol{x}_{t,j})\right)\varpi_j^{(r)}(t,i)\\
&-\frac{1}{2}\sum_{t=1}^{T_j}\boldsymbol{Q}_j^{-1}\left(\boldsymbol{x}_{t,j}-\boldsymbol{f}_t(\boldsymbol{x}_{t,j-1})\right)\\
&+\sum_{t=1}^{T_j}\log p\left(s_{t,j}|s_{t,j-1}\right)\Bigg|_{\substack{\boldsymbol{x}_{t,j}=\widehat{\boldsymbol{x}}_{t,j|k-l:k}(r+1)\\ s_{t,j}=\widehat{s}_{t,j|k-l:k}(r+1)}}=0 \quad (34)
\end{aligned}$$

where $\boldsymbol{H}_i$ represents the Jacobian matrix of $\boldsymbol{h}_i$.

3) Hybrid Forward–Backward Algorithm for Detection and Tracking: The problem (34) is difficult to solve. The reason is that it is a symmetric block tridiagonal nonlinear system and involves two unknown variable quantities. An approximate and algebraic manipulation-terse solution is present here.

The posterior probability mass function $p(s_{t,j|k-l:k})$ of target existence state is obtained by using a forward–backward algorithm

$$p(s_{t,j|k-l:k})=\frac{\alpha_j(s_{t,j})\beta_j(s_{t,j})}{\sum_{\gamma=0}^{1}\alpha_j(\gamma)\beta_j(\gamma)} \quad (35)$$

where

$$\begin{aligned}
\alpha_j(s_{t,j})=&\left(\sum_{\gamma=0}^{1}\alpha_{j-1}(\gamma)\pi_{s_{t,j-1}}(s_{t,j-1},\gamma)\right)\\
&\times\exp\left(\xi_{t,j-1}(s_{t,j-1})\right), \quad (36)\\
\beta_j(s_{t,j})=&\left(\sum_{\gamma=0}^{1}\beta_{j+1}(\gamma)\pi_{s_{t,j}}(s_{t,j},\gamma)\exp\left(\xi_{t,j}(\gamma)\right)\right) \quad (37)
\end{aligned}$$

$$\begin{aligned}
\xi_{t,j}(s_{t,j})=&\sum_{i=1}^{I}\left(1-\mathbb{E}\left[d_j^{t,i}(\boldsymbol{\Theta}_j)\right]\right)\log\left(1-p_d^i(s_{t,j})\right)\\
&+\sum_{i=1}^{I}\mathbb{E}\left[d_j^{t,i}\left(\boldsymbol{\Theta}_j\right)\right]\log p_d^i(s_{t,j}) \quad (38)
\end{aligned}$$

with $\mathbb{E}[d_j^{t,i}(\boldsymbol{\Theta}_k)]=\sum_{n=1}^{N_j}\mathbb{E}[\theta_j^{t,i,n}]$.

Then, putting (35) into (34), (34) is rewritten as

$$\begin{aligned}
&\sum_{t=1}^{T_j}\sum_{i=1}^{I}\log\left(\frac{(\lambda V_j)^{N_C(\boldsymbol{\Theta}_j)}}{N_j!}\exp(-\lambda V_j)\right.\\
&\left.\times\left(p_d^i(s_{t,j}(r))\right)^{d_j^{t,i}(\boldsymbol{\Theta}_j)}\left(1-p_d^i(s_{t,j}(r))\right)^{1-d_j^{t,i}(\boldsymbol{\Theta}_j)}\right)\\
&-\frac{1}{2}\sum_{t=1}^{T_j}\sum_{i=1}^{I}\left(\boldsymbol{H}_i(\boldsymbol{x}_{t,j})\right)^T\left(\tilde{\boldsymbol{R}}_j^{t,i}(r)\right)^{-1}\\
&\times\left(\tilde{\boldsymbol{z}}_j^{t,i}(r)-\boldsymbol{h}_i(\boldsymbol{x}_{t,j})\right)\varpi_j^{(r)}(t,i)\\
&-\frac{1}{2}\sum_{t=1}^{T_j}\boldsymbol{Q}_j^{-1}\left(\boldsymbol{x}_{t,j}-\boldsymbol{f}_t(\boldsymbol{x}_{t,j-1})\right)\\
&+\sum_{t=1}^{T_j}\log p\left(s_{t,j}|s_{t,j-1}\right)\Bigg|_{\boldsymbol{x}_{t,j}=\widehat{\boldsymbol{x}}_{t,j|k-l:k}(r+1)}=0. \quad (39)
\end{aligned}$$

The solution for state estimation is given

$$\widehat{\boldsymbol{x}}_{t,j|k-l:k}(r+1)=\frac{\sum_{i=1}^{I}\varpi_j^{(r)}(t,i)\left(\boldsymbol{\Phi}_{t,j|k-l:k}^{i}\right)^{-1}\widehat{\boldsymbol{x}}_{t,j|k-l:k}}{\sum_{i=1}^{I}\varpi_j^{(r)}(t,i)\left(\boldsymbol{\Phi}_{t,j|k-l:k}^{i}\right)^{-1}} \quad (40)$$

$$\boldsymbol{\Phi}_{t,j|k-l:k}(r+1)=\left(\sum_{i=1}^{I}\varpi_j^{(r)}(t,i)\left(\boldsymbol{\Phi}_{t,j|k-l:k}^{i}\right)^{-1}\right)^{-1} \quad (41)$$

where $\widehat{\boldsymbol{x}}_{t,j|k-l:k}^{i}$ and $\boldsymbol{\Phi}_{t,j|k-l:k}^{i}$ is the state smoothing of target t at time instant j via ith propagation mode. This is obtained through a fixed interval smoother [28], which consists of the forward and backward filtered outputs

$$\begin{aligned}
\widehat{\boldsymbol{x}}_{t,j|k-l:k}=&\boldsymbol{\Phi}_{t,j|k-l:k}^{i}\left[\left(\boldsymbol{\Phi}_{t,j|k-l:j}^{i}\right)^{-1}\widehat{\boldsymbol{x}}_{t,j|k-l:j}^{i}\right.\\
&\left.+\left(\boldsymbol{\Phi}_{t,j|j+1:k}^{i}\right)^{-1}\widehat{\boldsymbol{x}}_{t,j|j+1:k}^{i}\right] \quad (42)
\end{aligned}$$

$$\boldsymbol{\Phi}_{t,j|k-l:k}^{i}=\left[\left(\boldsymbol{\Phi}_{t,j|k-l:j}^{i}\right)^{-1}+\left(\boldsymbol{\Phi}_{t,j|j+1:k}^{i}\right)^{-1}\right]^{-1} \quad (43)$$

where the forward estimate $\widehat{\boldsymbol{x}}_{t,j|k-l:j}^{i}$, $\boldsymbol{\Phi}_{t,j|k-l:j}^{i}$ and the backward estimate $\widehat{\boldsymbol{x}}_{t|j+1;k}^{i}$, $\boldsymbol{\Phi}_{t,j|j+1:k}^{i}$ can be obtained by a filter such as unscented Kalman filter (UKF) or extended Kalman filter (EKF) [28], [29].

D. Initialization and Termination

1) Initialization: The initial target existence state, target kinematic state, and corresponding covariances need to be specified during the initialization of the JMDT-EM system. Having the great impact on the final tracking results, convergence speed, and robustness of the system, initialization values without proper specified will lead to serious tracking performance degradation. Based on K-means strategy utilizing on cluster results [26] and the stochastic initialization method by choosing the best one satisfy local maximum among different initial values, a combine

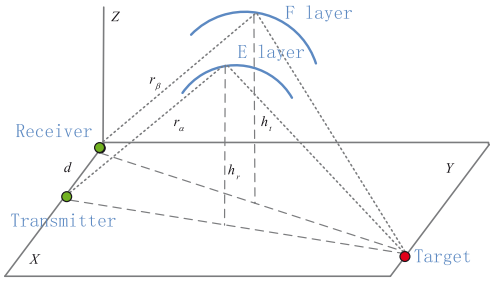

Fig. 2. Geometry of OTHR multipath propagation model.

method is used here. In the next section, we illustrate the detection and tracking results of the proposed JMDT-EM algorithm with both K-means strategy and stochastic initialization strategy.

2) Termination: One attractive property of the EM algorithm is the monotonicity of the log-likelihood function, which guarantees the algorithm can converge to a point of the posterior density. Thus, the iteration cycle will be terminated if the iterative number reaches a predetermined maximum iterations or the difference between two consecutive iteration cycle estimation results is less than a predetermined value. Notice that the computation and communication burdens increase linearly with iterative number; therefore a suitable tradeoff between performance and cost should be considered.

IV. Simulation

The proposed JMDT-EM algorithm applies any multitarget detection and tracking in the multipath environment in practical applications, such as the multipath effect of underwater sound transmission, multipath propagation phenomenon in skywave OTHR, and multipath effects in millimeter-wave wireless communication. In this section, the performance of the proposed JMDT-EM algorithm is evaluated based on the OTHR multitarget tracking scenario. For comparison, the performance of MD-PDAF, MD-MHT, and JDT-VB are also presented. The statistical results of the experimental group algorithm (JMDT-EM) and the control group algorithms (MD-PDAF, MD-MHT, and JDT-VB) are based on 400 Monte Carlo runs.

A. Simulation Scenario Setting

Assume that the simulation scenario of OTHR multitarget tracking involves six targets moving in the surveillance region and uses a two-layer (E layer and F layer) ionospheric model as [18]. The propagation model is determined by the system configuration and ionospheric model. Table I gives the details of the scenario parameter sets. Fig. 2 shows the geometry of OTHR multipath propagation model. The radar signal from the transmitter goes through the ionosphere, reflected by one of the two ionospheric layers, and reaches the target. After being scattered by the target, the signal returns through the ionosphere, reflected by one of the two ionospheric layers again, and finally reaches the receiver. Therefore, four propagation modes can be generated as follows:

1) EE: transmitted through E layer, received through E layer.
2) EF: transmitted through E layer, received through F layer.

TABLE I
Simulation Scenario Setting

number of modes	4
ionosphere height (h_E, h_F)	(100km,260km)
T-R distance d	100km
number of dwells	40
time between dwells	16 seconds
range region size	1500-2000km
azimuth region size	0.428-0.608rad
range rate region size	-0.524-0.524km/s
number of clutter N_c	400/125 points
process noise covariance $\boldsymbol{Q}$	$\boldsymbol{B}\left(\begin{bmatrix} 10^{-6} & 10^{-7} \\ 10^{-7} & 10^{-8} \end{bmatrix}, \begin{bmatrix} 10^{-9} & 10^{-10} \\ 10^{-10} & 10^{-11} \end{bmatrix}\right)$
noise covariances $\boldsymbol{R}_{i,k}$	$diag$(25,1e-6,9e-6)
measurement matrix $\boldsymbol{h}_i$	see Eq. (44)
gate probability P_g	0.971
initial track confidence	0.2
track existence	0.8
track deletion	0.3
window length l	5 dwells
threshold of iterative termination δ_L	1e-5
maximum iterative number r_{max}	10

Note: $\otimes$ denotes the kronecker product; $\boldsymbol{B}(\cdot)$ denotes blockdiag; $\boldsymbol{R}_{i,k}$ are in km^2, (km/s)^2, (rad)^2.

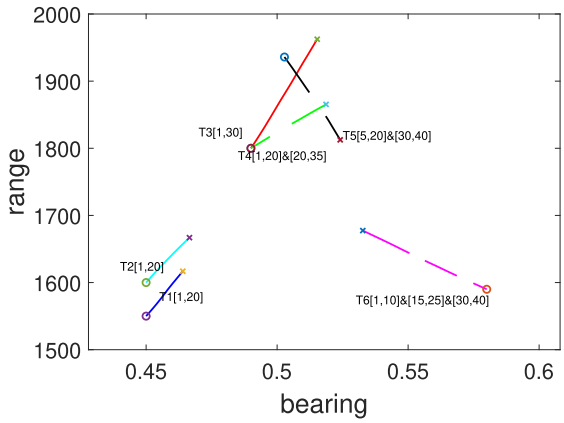

Fig. 3. Targets tracking trajectories and lifetime in ground coordinate system.

3) FE: transmitted through F layer, received through E layer.
4) FF: transmitted through F layer, received through F layer.

The look-up table for details of target kinematic state information and lifetime information refers to Table II.

Note that the OTHR target kinematic state $\boldsymbol{x}_k$ consists of ground range ρ_k, ground range rate $\dot{\rho}_k$, bearing b_k, and bearing rate $\dot{b}_k$ in ground coordinates. Target-originated measurement z_k consists of slant range r_k, slant range rate $\dot{r}_k$, and azimuth ψ_k in slant coordinates. The measurement function which involves the mapping from $\boldsymbol{x}_k$ to $\boldsymbol{z}_k$ is given by [12]

$$\begin{aligned} r_k &= r_{\alpha,k} + r_{\beta,k} \\ \dot{r}_k &= \frac{\dot{\rho}_k}{4}\left(\frac{\rho_k}{r_{\alpha,k}} + \frac{\rho_k - d\sin(b_k)}{r_{\beta,k}}\right) \\ \psi_k &= \arcsin\left(\frac{\rho_k \sin(b_k)}{2r_{\alpha,k}}\right) \end{aligned} \tag{44}$$

TABLE II
PARAMETERS SETTINGS OF THE TARGETS

Category	Target initial state	Lifetime	STM $\boldsymbol{F}$	TCTM	$\Sigma_{0\|0}$
Target 1	(1550,0.22,0.45,5.0e-5)	[1,20]	$I_2 \otimes \begin{bmatrix} 1 & 16 \\ 0 & 1 \end{bmatrix}$	$\begin{bmatrix} 0.75 & 0.25 \\ 0.05 & 0.95 \end{bmatrix}$	$diag$(25,1e-6,9e-6,4.5e-8)
Target 2	(1600,0.22,0.45,5.0e-5)	[1,20]	$I_2 \otimes \begin{bmatrix} 1 & 32 \\ 0 & 1 \end{bmatrix}$	$\begin{bmatrix} 0.75 & 0.25 \\ 0.05 & 0.95 \end{bmatrix}$	$diag$(25,1e-6,9e-6,4.5e-8)
Target 3	(1800,0.35,0.49,6.0e-5)	[1,30]	$I_2 \otimes \begin{bmatrix} 1 & 25 \\ 0 & 1 \end{bmatrix}$	$\begin{bmatrix} 0.85 & 0.15 \\ 0.15 & 0.85 \end{bmatrix}$	$diag$(25,1e-6,9e-6,4.5e-8)
Target 4	(1800,0.22,0.50,4.5e-5)	[1,10]&[20,35]	$I_2 \otimes \begin{bmatrix} 1 & 16 \\ 0 & 1 \end{bmatrix}$	$\begin{bmatrix} 0.85 & 0.15 \\ 0.15 & 0.85 \end{bmatrix}$	$diag$(25,1e-6,9e-6,4.5e-8)
Target 5	(1950,-0.22,0.50,4.5e-5)	[5,20]&[30,40]	$I_2 \otimes \begin{bmatrix} 1 & 20 \\ 0 & 1 \end{bmatrix}$	$\begin{bmatrix} 0.85 & 0.15 \\ 0.15 & 0.85 \end{bmatrix}$	$diag$(25,1e-6,9e-6,4.5e-8)
Target 6	(1590,0.14,0.58,-8e-5)	[1,10]&[15,25]&[30,40]	$I_2 \otimes \begin{bmatrix} 1 & 16 \\ 0 & 1 \end{bmatrix}$	$\begin{bmatrix} 0.65 & 0.35 \\ 0.35 & 0.65 \end{bmatrix}$	$diag$(25,1e-6,9e-6,4.5e-8)

Note: Target initial state consist of range, range rate, bearing and bearing rate in km, km/s, rad, and rad/s, respectively. $\mathbf{STM}$ and $\mathbf{TCTM}$ represent target state transition matrix and target state confident transition matrix, respectively. $\Sigma_{0|0}$ represents targets represents target initial state covariance.

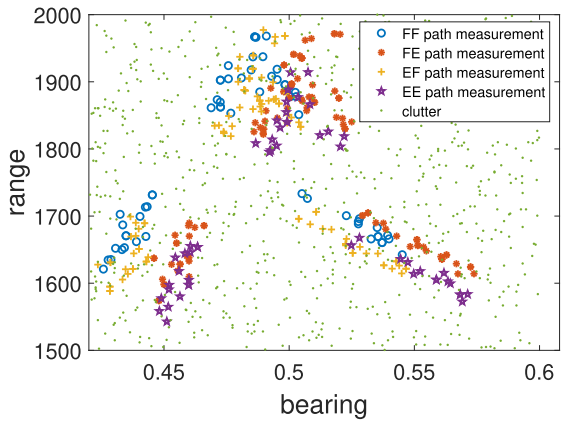

Fig. 4. Multipath measurements and clutter in slant coordinate system.

with

$$r_{\alpha,k} = \sqrt{\frac{\rho_k^2}{4} + h_r^2}$$
$$r_{\beta,k} = \sqrt{\frac{\rho_k^2 - 2d\rho_k \sin b_k + d^2}{4} + h_t^2} \tag{45}$$

where $r_{\alpha,k}$ and $r_{\beta,k}$ denote the ranges of transmitter and receiver, respectively. d represents the distance between the transmitter and the receiver. Instead of linearization required by the EKF, we use the UKF to estimate target state in this article.

B. Performance Measures

In order to evaluate the proposed algorithm and its control group algorithms, Three classes of metrics are taken into consideration: track cardinality measures, time metrics, and track accuracy [30], [31].

1) Track Cardinality Measures: (a) Number of valid tracks (NVT ↑): If a track is associated to only one target and the associated target is only assigned to the only track. (b) Number of false tracks (NFT ↓): If a track is not associated to any target. (c) Number of missed targets (NMT ↓): If a target is not associated to any track.

2) Time Metrics: (d)Track probability of detection (TPD ↑): The radio of the duration that a target is assigned to a valid track to the duration that the target is present. (e) Total execution time (TET ↓): The total time needed to run the tracker.

3) Track Accuracy: (f) Error in ground range (EGR ↓). (g) Error in range rate (ERR ↓). (g) Error in bearing (EB ↓). (i) Error in bearing rate (EBR ↓).

Notation: ↑ (↓) represents the higher (lower) the measure, the better the performance.

C. Performance Analysis

Fig. 3 shows the true trajectories and corresponding lifetime in ground coordinate system. The start and end point of a target are denoted by ∘ and ×, respectively. $T_t[k1, k2]$ denotes that target t appears at time instant $k1$ and disappears at time instant $k2$. Fig. 4 shows the clutter and multipath target-originated measurements in slant coordinate when $p_d^1 = p_d^4 = 0.4$, $p_d^2 = p_d^3 = 0.7$, and $N_c = 125$.

Fig. 5 shows the tracking trajectories obtained by MD-PDAF, MD-MHT, JDT-VB, and JMDT-EM. Fig. 5(a)–(d) illustrates the tracking results with $p_d^1 = p_d^4 = 0.4$, $p_d^2 = p_d^3 = 0.7$ and $N_c = 125$. As we can see from Fig. 5(a), all targets are successfully tracked. However, during the MD-PDAF process, some false tracks from clutter and ghost tracks of target 3 and target 4 appear as well. It can be seen from Fig. 5(b) that although MD-MHT tracks all targets, there are still some ghost track of target 3, 4, and 5. Besides, some tracks corresponding to target 6 are lost. Fig. 5(c) shows that JDT-VB tracks all targets more accuracy than MD-PDAF and MD-MHT. From Fig. 5(d), we can see that JMDT-EM can track all the targets successfully and achieves better estimation accuracy than related MD-PDAF, MD-MHT, and JDT-VB when compare transient and steady state performance. Fig. 5(e)–(h) obtained under the configuration $p_d^1 = p_d^2 = p_d^3 = p_d^4 = 0.4$ and $N_c = 400$. It can be seen that all the targets are successfully tracked, which is the same as the results illustrate in Fig. 5(a)–(d). However, MD-PDAF and MD-MHT suffer serious performance degradation. More false tracks from clutter and ghost tracks of target 3, 4, and 5 appear in Fig. 5(e) than that in Fig. 5(a). From Fig. 5(f), it

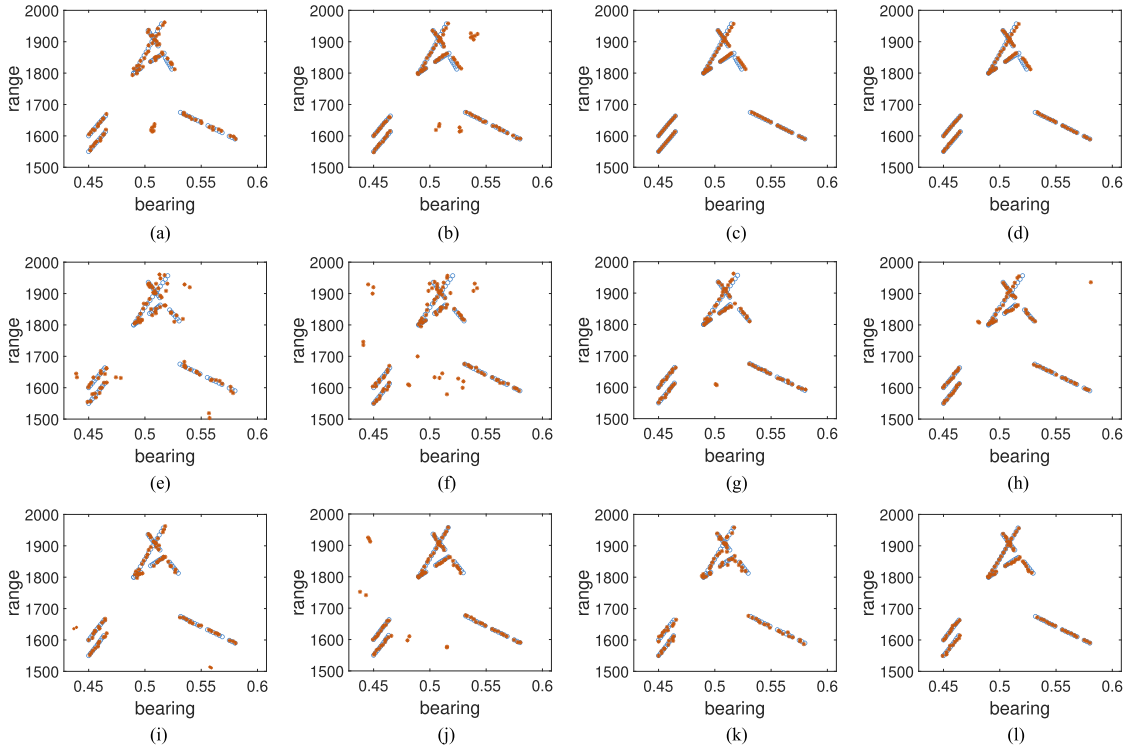

Fig. 5. Tracking trajectories obtained by MD-PDAF, MD-MHT, JDT-VB, and JMDT-EM (The blue ○ denotes the real target moving strategy and the orange ∗ denotes the tracking results).

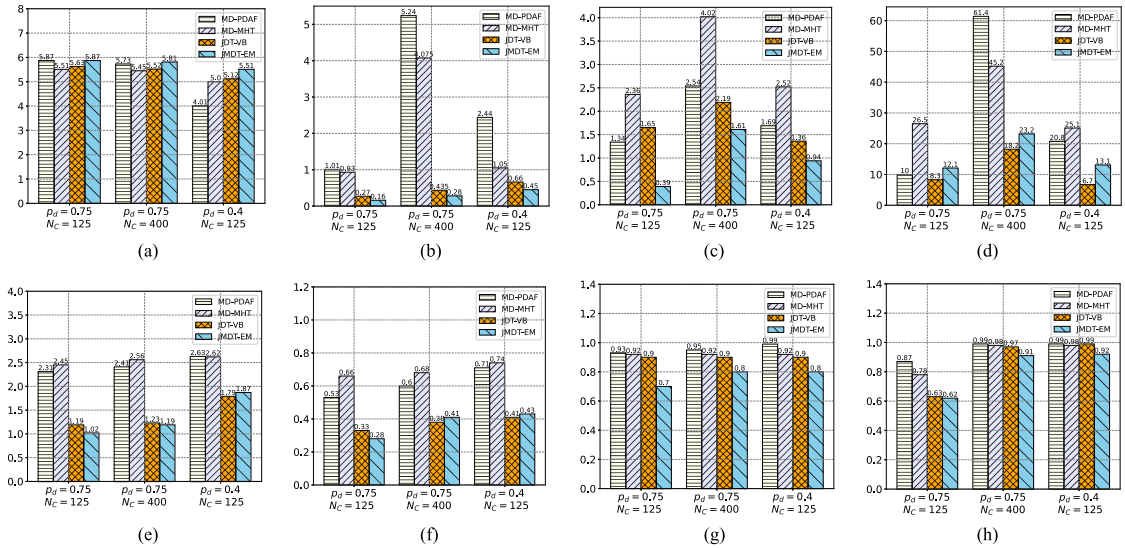

Fig. 6. Performance Measures for MD-PDAF, MD-MHT, JDT-VB, and JMDT-EM.

can be seen more ghost tracks appear and more tracks are lost than that from Fig. 5(b). JDT-VB and JMDT-EM also suffer some performance degradation, which can be seen in Fig. 5(g)–(h). Fig. 5(i)–(l) have the same configuration with Fig. 5(a)–(d) that $p_d^1 = p_d^4 = 0.4$, $p_d^2 = p_d^3 = 0.7$, and $N_c = 125$, except with single element subsets initialization. It can be seen from Fig. 5(k) that without proper initialization, JDT-VB has more ghost tracks in the first few scans and there are also some tracks lost, while JMDT-EM can still remain satisfying tracking performance.

Fig. 6 provides the statistical results of MD-PDAF, MD-MHT, JDT-VB, and JMDT-EM with different path detection probability and clutter configuration. As expected, less clutter and higher detection probability lead to better tracking performance. Particularly, in the matter of NVT, JMDT-EM performs best and most robust with respect to detection probability than MD-PDAF, MD-MHT, and JDT-VB. However, MD-PDAF performs dramatically with the detection probability. JDT-VB and MD-MHT have similar track detection performance which are more robust than MD-PDAF with different detection probability. In terms of

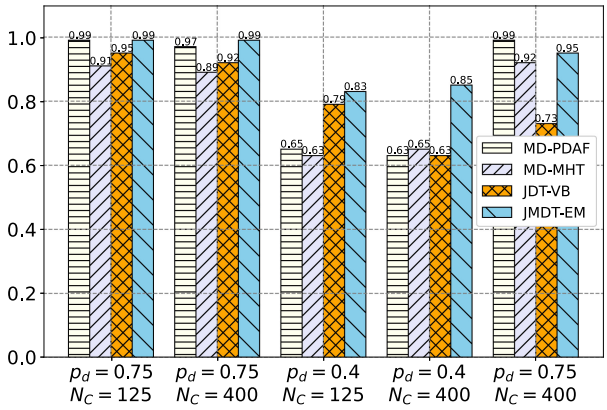

Fig. 7. Detection performance of MD-PDAF, MD-MHT, JDT-VB, and JMDT-EM.

NFT, the performance of JMDT-EM and JDT-VB is much better than those of MD-MHT and MD-PDAF. The advantages are more obvious especially in large number of clutter case. In the aspect of NMT, MD-MHT, and JDT-VB have worse performance than MD-PDAF and JMDT-EM, which is due to low detection probability and inappropriate track initialization. In terms of TET, MD-MHT is much better than MD-PDAF, JDT-VB, and JMDT-EM in the large number clutter case. However, the TET of JDT-VB increases dramatically with larger number clutter, which is caused by track initialization. In terms of the tracking error, the performance of MD-PDAF is worse than those of JMDT-EM, JDT-VB, and MD-HMHT. The reason is that based on the track-level fusion framework MD-PDAF suffers more performance degradation compared with the measurement-level fusion based frameworks.

Fig. 7 provides the statistical results on TPD. The last column has the same parameter settings as the first one except without proper initialization values. Fig. 7 shows that JMDT-EM performs slightly better than JDT-VB, and outperforms MD-PDAF and MD-MHT, which due to information fusion at measurement level to avoid information loss. Furthermore, by using different initial values, it can be seen that JMDT-EM is more robust than JDT-VB.

These extensive simulations verify that the proposed JMDT-EM exhibits excellent performance in the presence of incomplete data situation and get an appropriate trade-off between diverse motion situations and estimation performance.

V. Conclusion

In this article, we have addressed the problem of joint detection and tracking for multitarget in multipath environment. A joint optimation detection and tracking algorithm (JMDT-EM) based on EM approach is present. The proposed scheme iteratively optimizes estimation and data association by alternately estimating the missing data in E-step and optimizing target state in M-step. Furthermore, the proposed scheme also provides a hybrid forward and backward algorithm to solve the coupling of target existence state and target kinematic state. A convergence speed up algorithm based on K-means strategy and stochastic initialization strategy is also provided. Finally, the experimental results show that the proposed algorithm achieves a better detection and tracking performance than existing methods but also stays stable performance in complex and changeable motion environment and low SNR circumstance.

Appendix A

The log-likelihood function $\mathcal{L}_{k-l}^{k}$ is written as follows:

$$\begin{aligned}\mathcal{L}_{k-l}^{k} &= \log\left(p\left(\boldsymbol{X}_{k-l}^{k}, \boldsymbol{S}_{k-l}^{k}, \boldsymbol{Z}_{k-l}^{k}, \boldsymbol{\Theta}_{k-l}^{k} | \boldsymbol{Z}_{1}^{k-l-1}\right)\right) \\ &= \sum_{j=k-l}^{k} \log\left(p\left(\boldsymbol{Z}_j | \boldsymbol{X}_j, \boldsymbol{\Theta}_j, \boldsymbol{S}_j\right)\right) \\ &\quad + \sum_{j=k-l}^{k} \log\left(p\left(\boldsymbol{X}_j | \boldsymbol{X}_{j-1}\right)\right) \\ &\quad + \log\left(p\left(\boldsymbol{X}_{k-l-1} | \boldsymbol{Z}_{1}^{k-l-1}\right)\right) \\ &\quad + \sum_{j=k-l}^{k} \log\left(p(\boldsymbol{\Theta}_j | \boldsymbol{S}_j)\right) \\ &\quad + \sum_{j=k-l}^{k} \log\left(p\left(\boldsymbol{S}_j | \boldsymbol{S}_{j-1}\right)\right) \\ &\quad + \log\left(p\left(\boldsymbol{S}_{k-l-1}\right)\right) \end{aligned} \tag{46}$$

where the PDF of $\boldsymbol{x}_{k-l-1}$, $\boldsymbol{x}_j$ and $\boldsymbol{z}_j^i(n)$ are all Gaussian. Thus

$$\begin{aligned} p\left(\boldsymbol{X}_j | \boldsymbol{X}_{j-1}\right) &= \prod_{t=1}^{T_j} p\left(\boldsymbol{x}_j^t | \boldsymbol{x}^t{}_{j-1}\right) \\ &= \prod_{t=1}^{T_j} N\left(\boldsymbol{x}_j^t; \boldsymbol{f}^t(\boldsymbol{x}_{j-1}^t), \boldsymbol{Q}_j^t\right) \end{aligned} \tag{47}$$

$$\begin{aligned} p\left(\boldsymbol{X}_{k-l-1} | \boldsymbol{Z}_{1}^{k-l-1}\right) &= \prod_{t=1}^{T_j} p\left(\boldsymbol{x}_{k-l-1}^t | \boldsymbol{z}_{k-l-1}^t\right) \\ &= \prod_{t=1}^{T_j} N\left(\boldsymbol{x}_{k-l-1}^t; \widehat{\boldsymbol{x}}_{k-l-1}^t, \boldsymbol{\Sigma}_{k-l-1}\right) \end{aligned} \tag{48}$$

$$p\left(\boldsymbol{Z}_j | \boldsymbol{X}_j, \boldsymbol{\Theta}_j, \boldsymbol{S}_j\right) = \begin{cases} (V_j)^{-d_j^{t,i}(\boldsymbol{\Theta}_j)+1} p\left(\boldsymbol{Z}_j | \boldsymbol{X}_j, \boldsymbol{\Theta}_j\right), & \theta_j^{t,i,n} \in \boldsymbol{\theta}'_j \\ (V_j)^{-d_j^{t,i}(\boldsymbol{\Theta}_j)}, & others \end{cases} \tag{49}$$

where

$$\begin{aligned} p\left(\boldsymbol{Z}_j | \boldsymbol{X}_j, \boldsymbol{\Theta}_j\right) &= \prod_{t=1}^{T_j} p\left(\boldsymbol{z}_j^t | \boldsymbol{x}_j^t\right) \\ &= \prod_{t=1}^{T_j} N\left(\boldsymbol{z}_j; \boldsymbol{h}^i(\boldsymbol{x}_j^t), \boldsymbol{R}_j^i\right). \end{aligned} \tag{50}$$

The relationship between the target existence state and data association event $\boldsymbol{\Theta}_j$ is tightly coupled.

$$p(\boldsymbol{\Theta}_j|\boldsymbol{s}_j) = \frac{(\lambda V_j)^{\left(N_j-\sum_{t=1}^{T_j}\sum_{i=1}^{I} d^{t,i}(\boldsymbol{\Theta}_j)\right)}}{N_j!}\exp(-\lambda V_j) \cdot \prod_{t=1}^{T_j}\prod_{i=1}^{I}\left(p_d^i(s_{t,j})\right)^{d_j^{t,i}(\boldsymbol{\Theta}_j)}\left(1-p_d^i(s_{t,j})\right)^{1-d_j^{t,i}(\boldsymbol{\Theta}_j)} \quad (51)$$

$d^{t,i}(\boldsymbol{\Theta}_j)$ is the detection indicator that denotes whether a measurement is assigned with target t propagation via path i. $p_d^i(s_{t,k})$ denotes the target existence state-dependent detection probability for each target t via each propagation path i.

APPENDIX B

According to (9), the $\mathcal{Q}$-function is given as follows:

$$\begin{aligned}\mathcal{Q}_{k-l}^k(r) &= \mathbb{E}\left(\mathcal{L}_{k-l}^k|\boldsymbol{Z}_{k-l}^k, \widehat{\boldsymbol{X}}_{k-l}^k(r), \widehat{\boldsymbol{S}}_{k-l}^k(r)\right)\\ &= \mathbb{E}\left(\mathcal{L}_{1,k-l}^k|\boldsymbol{Z}_{k-l}^k, \widehat{\boldsymbol{X}}_{k-l}^k(r), \widehat{\boldsymbol{S}}_{k-l}^k(r)\right)\\ &\quad + \mathbb{E}\left(\mathcal{L}_{2,k-l}^k|\boldsymbol{Z}_{k-l}^k, \widehat{\boldsymbol{X}}_{k-l}^k(r), \widehat{\boldsymbol{S}}_{k-l}^k(r)\right)\\ &\quad + \mathbb{E}\left(\mathcal{L}_{3,k-l}^k|\boldsymbol{Z}_{k-l}^k, \widehat{\boldsymbol{X}}_{k-l}^k(r), \widehat{\boldsymbol{S}}_{k-l}^k(r)\right)\\ &\quad + \mathbb{E}\left(\mathcal{L}_{4,k-l}^k|\boldsymbol{Z}_{k-l}^k, \widehat{\boldsymbol{X}}_{k-l}^k(r), \widehat{\boldsymbol{S}}_{k-l}^k(r)\right). \quad (52)\end{aligned}$$

Through putting (17)–(21) into (52), the $\mathcal{Q}$-function is rewritten as

$$\mathcal{Q}_{k-l}^k(r) = \mathcal{Q}_{1,k-l}^k + \mathcal{Q}_{2,k-l}^k + \mathcal{Q}_{3,k-l}^k + \mathcal{Q}_{4,k-l}^k \quad (53)$$

with

$$\begin{aligned}\mathcal{Q}_{1,k-l}^k =& -\frac{1}{2}\sum_{j=k-l}^{k}\sum_{t=1}^{T_j}\log\left(\left|2\pi\boldsymbol{Q}_{t,j}\right|\right)\\ &-\frac{1}{2}\sum_{j=k-l}^{k}\sum_{t=1}^{T_j}\mathbf{D}\left(\boldsymbol{x}_{t,j}-\boldsymbol{f}_t\left(\boldsymbol{x}_{t,j-1}\right),\boldsymbol{Q}_{t,j}\right)\end{aligned}$$

$$\begin{aligned}\mathcal{Q}_{2,k-l}^k =& -\frac{1}{2}\sum_{t=1}^{T_\varsigma}\log\left(\left|2\pi\boldsymbol{\Sigma}_{t,\varsigma,\varsigma|1:\varsigma}\right|\right)\\ &-\frac{1}{2}\sum_{t=1}^{T_\varsigma}\mathbf{D}\left(\boldsymbol{x}_{t,\varsigma}-\widehat{\boldsymbol{x}}_{t,\varsigma|1:\varsigma},\boldsymbol{\Sigma}_{t,\varsigma,\varsigma|1:\varsigma}\right)\end{aligned}$$

$$\begin{aligned}\mathcal{Q}_{3,k-l}^k =& \Bigg(-\frac{1}{2}\sum_{j=k-l}^{k}\sum_{t=1}^{T_j}\sum_{i=1}^{I}\sum_{n:\boldsymbol{z}_{n,j}\in V_j(\eta)}\\ &\left(\log\left(\left|2\pi\boldsymbol{R}_{i,j}\right|\right)+\mathbf{D}\left(\boldsymbol{z}_j-\boldsymbol{h}_i\left(\boldsymbol{x}_{t,j}\right),\boldsymbol{R}_{i,j}\right)\right)\\ &+\sum_{j=k-l}^{k}\left(1-\delta(\boldsymbol{\Theta}_j)\right)\log\left(V_j\right)\Bigg)\\ &\times p\left(\theta_j^{t,i,n}\in\boldsymbol{\theta}_j'|\boldsymbol{Z}_{k-l}^k,\widehat{\boldsymbol{X}}_{k-l}^k(r),\widehat{\boldsymbol{S}}_{k-l}^k(r)\right)\end{aligned}$$

$$\begin{aligned}\mathcal{Q}_{4,k-l}^k =& \sum_{j=k-l}^{k}\log p(\boldsymbol{\Theta}_j|\boldsymbol{s}_j)+\sum_{j=k-l}^{k}\log p\left(\boldsymbol{s}_j|\boldsymbol{s}_{j-1}\right)\\ &+\log p(\boldsymbol{s}_\varsigma).\end{aligned}$$

where $p(\theta_j^{t,i,n}\in\boldsymbol{\theta}_j'|\boldsymbol{Z}_{k-l}^k,\widehat{\boldsymbol{X}}_{k-l}^k(r),\widehat{\boldsymbol{S}}_{k-l}^k(r))$ is given in (28).

REFERENCES

[1] Y. Bar-Shalom and X. R. Li, "Multitarget multisensor tracking: Principles and techniques," *IEEE Aerosp. Electron. Syst. Mag.*, vol. 16, no. 1, p. 93, Feb. 1996.

[2] G. W. Pulford, "Taxonomy of multiple target tracking methods," *IEEE Proc. Radar, Sonar Navigat.*, vol. 152, no. 5, pp. 291–304, Nov. 2005.

[3] X. Y. Liu *et al.*, "CDC: Compressive data collection for wireless sensor networks," *IEEE Trans. Parallel Distrib. Syst.*, vol. 26, no. 8, pp. 2188–2197, Aug. 2015.

[4] C. Gao, H. Liu, S. H. Zhou, H. T. Su and J. K. Yan, "Maneuvering target tracking with recurrent neural networks for radar application," in *Proc. Int. Conf. Radar*, 2018, pp. 1–5.

[5] L. Kong *et al.*, "Data loss and reconstruction in wireless sensor networks," *IEEE Trans. Parallel Distrib. Syst.*, vol. 25, no. 11, pp. 2818–2828, Nov. 2014.

[6] Z. H. Li, H. T. Su, S. H. Zhou and Q. Z. Hu, "Signal fusion-based targets detection in the presence of clutter and subspace interference for multiple-input-multiple-output radar," *IET Radar, Sonar Navigat.*. vol. 13, no. 1, pp. 148–155, Jan. 2019.

[7] K. Granstrom, M. Baum, and R. Stephan, "Extended object tracking: Introduction, overview and applications," *J. Adv. Inf. Fusion*, vol. 12, pp. 1–18, 2016.

[8] M. Zhou, J. J. Zhang, and A. PapandreouSuppappola, "Multiple target tracking in urban environments," *IEEE Trans. Signal Process.*, vol. 64, no. 5, pp. 1270–1279, Mar. 2016.

[9] L. Li and J. L. Krolik, "Simultaneous target and multipath positioning," *IEEE J. Sel. Topics Signal Process.*, vol. 8, no. 1, pp. 153–165, Feb. 2014.

[10] S. J. Davey, G. A. Fabrizio and M. G. Rutten, "Detection and tracking of multipath targets in over-the horizon radar," *IEEE Trans. Aerosp. Electron. Syst.*, vol. 55, no. 5, pp. 2277–2295, Nov. 2018.

[11] T. Sathyan, T. J. Chin, S. Arulampalam, and D. Suter, "Amultiple hypothesis tracker for multitarget tracking with multiple simultaneous measurements," *IEEE J. Sel. Topics Signal Process.*, vol. 7, no. 3, pp. 448–460, Jun. 2013.

[12] G. W. Pulford, "OTHR multipath tracking with uncertain coordinate registration," *IEEE Trans. Aerosp. Electron. Syst.*, vol. 40, no. 1, pp. 38–56, Jan. 2004.

[13] X. Tang, X. Chen, M. McDonald, R. Mahler, R. Tharmarasa and T. Kirubarajan, "A multiple-detection probability hypothesis density filter," *IEEE Trans. Signal Process.*, vol. 63, no. 8, pp. 2007–2019, Apr. 2015.

[14] B. Habtemariam, R. Tharmarasa, T. Thayaparan, M. Mallick, and T. Kirubarajan, "A multiple detection joint probabilistic data association filter," *IEEE J. Sel. Topics Signal Process.*, vol. 7, no. 3, pp. 461–471, Jun. 2013.

[15] K. C. Chang and Y. B. Shalom, "Joint probabilistic data association for multitarget tracking with possibly unresolved measurements and maneuvers," *IEEE Trans. Autom. Control*, vol. 29, no. 7, pp. 585–594, Jul. 1984.

[16] M. L'azaro-Gredilla, S. V. Vaerenbergh and N. D. Lawrence, "Overlapping mixtures of Gaussian processes for the data association problem," *Pattern Recognit.*, vol. 45, no. 4, pp. 1386–1395, 2012.

[17] L. Zheng and X. Wang, "Improved multiple hypothesis tracker for joint multiple target tracking and feature extraction," *IEEE Trans. Aerosp. Electron. Syst.*, vol. 55. no. 6, pp. 3080–3089, Dec. 2019.

[18] T. Sathyan, T. JunChin, S. Arulampalam, and D. Suter, "A multiple hypothesis tracker for multitarget tracking with multiple simultaneous measurements," *IEEE J. Sel. Topics Signal Process.*, vol. 7, no. 3, pp. 448–460, Jun. 2013.

[19] X. Tang, X. Chen, M. McDonald, R. Mahler, R. Tharmarasa, and T. Kirubarajan, "A multiple detection probability hypothesis density filter," *IEEE Trans. Signal Process.*, vol. 63, no. 8, pp. 2007–2019, Apr. 2015.

[20] T. De Laet, H. Bruyninckx, and J. De Schutter, "Shape-based online multitarget tracking and detection for targets causing multiple measurements: Variational bayesian clustering and lossless data association," *IEEE Trans. Pattern Anal. Mach. Intell.*, vol. 33, no. 12, pp. 2477–2491, Dec. 2011.
[21] H. Lan, S. Sun, Z. Wang, Q. Pan and Z. Zhang, "Joint target detection and tracking in multipath environment: A variational Bayesian approach," *IEEE Trans. Aerosp. Electron. Syst.*, vol. 56, no. 3, pp. 2136–2156. Jun. 2020.
[22] M. Ye, J. Shen, G. Lin, T. Xiang, L. Shao and S. C. H. Hoi, "Deep learning for person re-identification: A survey and outlook," in *IEEE Trans. Pattern Anal. Mach. Intell.*, to be published, Jan. 2021, doi: 10.1109/TPAMI.2021.3054775.
[23] M. Ye, J. Shen, X. Zhang, P. C. Yuen and S.-F. Chang, "Augmentation invariant and instance spreading feature for softmax embedding," *IIEEE Trans. Pattern Anal. Mach. Intell.*, to be published, Aug. 2020, doi: 10.1109/TPAMI.2020.3013379.
[24] G. McLachlan and T. Krishnan, *The EM Algorithm and Extensions*, 2nd ed. New York, NY, USA: Wiley, 2008.
[25] M. V. Akinin, A. V. Akinina, A. V. Sokolov and A. S. Tarasov, "Application of EM algorithm in problems of pattern recognition on satellite images," in *Proc. 6th Mediterranean Conf. Embedded Comput.*, 2017, pp. 1–4.
[26] S. H. Yan, L. Y. Li, Z. Y. Fei and H. Xu, "Accelerating EM missing data filling algorithm based on the k-means," in *Proc. 4th Annu. Int. Conf. Netw. Inf. Syst. Comput.*, 2018, pp. 401–406.
[27] H. Lan, Y. Liang, Z. Wang, F. Yang, and Q. Pan, "Distributed ECM algorithm for OTHR multipath target tracking with unknown ionospheric heights," *IEEE J. Sel. Topics Signal Precss.*, vol. 12, no. 1, pp. 61–75, Feb. 2018.
[28] G. Wang, Y. Zhang and X. Wang, "Maximum correntropy rauch-tung-striebel smoother for nonlinear and non-Gaussian systems," *IEEE Trans. Autom. Control*, vol. 66, no. 3, pp. 1270–1277, Mar. 2021.
[29] G. Wang, Y. Zhang, and X. Wang, "Iterated maximum correntropy unscented Kalman filters for non-Gaussian systems," *Signal Process.*, vol. 163, pp. 87–94, May 2019.
[30] D. Schuhmacher, B. T. Vo, and B. N. Vo, "A consistent metric for performance evaluation of multi-object filters," *IEEE Trans. Signal Process.*, vol. 56, no. 8, pp. 3447–3457, Aug. 2008.
[31] A. A. Gorji, R. Tharmarasa and T. Kirubarajan, "Performance measures for multiple target tracking problems," in *Proc. 14th Int. Conf. Inf. Fusion*, 2011, pp. 1–8.

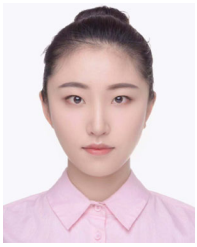

Zhihua Li (Student Member, IEEE) currently working toward the Ph.D. degree in signal and information processing with the National Key Laboratory of Radar Signal Processing, Xidian University, Xi'an, China.

She was a Visiting Scholar with the Electrical Engineering Department, Columbia University, NY, USA from October 2018 to May 2020. Her main research interests are in the fields of OTHR signal processing, adaptive target detection, and statistical signal processing.

Hongtao Su received the B.Eng., M.Eng., and Ph.D. degrees in electronic engineering from Xidian University, Xi'an, China, in 1997, 2000, and 2005, respectively.

He is currently a Professor with the National Key Laboratory of Radar Signal Processing, Xidian University. His main research interests are in the fields of HF OTHR signal processing, adaptive array signal processing, and statistical signal processing.

Xiao-Yang Liu (Graduate Student Member, IEEE) He received the Ph.D. degree in computer science from Shanghai Jiao Tong University, Shanghai, China, in 2016, the M.S. degree in electrical engineering from Columbia University, New York, NY, USA, in 2017, and the Ph.D. degree in electrical engineering from Columbia University, in 2020.

He is currently a Post Doctorate with the Department of Electrical Engineering, Columbia University. His research interests include tensor theory, non-convex optimization, deep learning, Big Data analysis, and data privacy.

Guoqing Wang received the B. S. degree from China University of Mining and Technology (CUMT), Xuzhou, China, in 2014, and the Ph.D. degree from Harbin Engineering University, Harbin, China, in 2019.

From October 2017 to May 2019, he has been a Visiting Scholar with the Electrical Engineering Department, Columbia University, New York, NY, USA. He is currently an Associate Professor with CUMT. His research interests focus on state estimation, information fusion, and their applications in navigation technology.

Mengdao Xing (Fellow, IEEE) he was born in Zhejiang, China, in November 1975. He received the B.S. and Ph.D. degrees in electrical engineering from Xidian University, Xi'an, China, in 1997 and 2002, respectively.

He is currently a Full Professor with the Academy of Advanced Interdisciplinary Research, Xidian University. He is also with the National Key Laboratory of Microwave Imaging Technology, Institute of Electronics, Chinese Academy of Sciences, Beijing, China. He has authored or coauthored two books and more than 200 papers. His research interests include synthetic aperture radar, inverse SAR, and sparse signal processing.